

## **URANIUM POTENTIALITY AND ITS EXTRACTION FROM EL SELA SHEAR ZONE, SOUTH EASTERN DESERT EGYPT.**

IBRAHIM, T. M.M.; AMER, T. E.; ALI, K. G.. and OMAR, S. M.  
Nuclear Materials Authority, P.O.Box 530 Maadi, Cairo, Egypt

### **ABSTRACT**

Due to the U-fertility criteria applied to El Sela granite pluton in the south Eastern Desert of Egypt, some mineralized zones were outlined for intensive work. The ENE-WSW structural trend was delineated as the master controlling fracture for the uranium mineralization in the area. This trend was intruded by micro-granite, multi-phases silica injections, basic and lamprophyre dykes associated with high potential fluid phases. Moreover, this trend acts as paleo-channel for the mineralized fluids and consequently control the alteration processes. Manual trenches have been excavated perpendicular to the main structural trend, samples were collected for scanning to detect the U-hosting minerals. Primary and secondary uranium minerals as well as uranium hosting minerals were identified and analyzed using microprobe to define their fertility.

to complete this study, hydrometallurgical experiments were carried out to test the leachability and the amount of extractable uranium from such ore material. For this purpose, a technological representative sample assaying about 0.095 % U was chosen for studying the leaching characteristics and the recovering conditions of U from the obtained leach liquors using anionic exchange resin. Many aspects of the leaching and recovery of U incorporated within this rock material have been obtained. The obtained product is in the form of  $\text{Na}_2\text{U}_2\text{O}_7$ . In addition, a tentative flowsheet was proposed and described.

### **INTRODUCTION**

El Sela area is located in the southern Eastern Desert of Egypt, between Latitudes  $22^\circ 14' 30''$  and  $22^\circ 18' 36''$  N and Longitudes  $36^\circ 11' 45''$  and  $36^\circ 16' 30''$  E. It is about 30 km south west of Abu Ramad City and occupies about 73.5  $\text{km}^2$  (Fig. -1).

Recent studies show increasingly that El Sela granite pluton is composed of multiple magma and other injection phases of various sizes and variable metallogenic potentialities typically like Kab Amiri granite plutons in the Eastern

Ibrahim, T.M.M. et al.

Desert of Egypt (Abdel Meguid et al. 2003). Such conception indicates that mineralization may be genetically related to only specific magma intrusion within a large granite complex as described in El Missikat granite central Eastern Desert of Egypt (Ibrahim, 2002). and Saint Sylvester granite in the French Central Massif for vein type uranium mineralization (Cuney et al. 1990). The ENE-WSE structural trend that crosscut El Sela granite is separated as the most U-fertile zone in the area. This study aims to illuminate the important uranium minerals and the optimum conditions for their recovery.

The fertility of a granitic pluton is mostly related to the extent of the overlap between the magmatic uranium enrichment, hydrothermal reworking through an open fracture system and suitable reservoir for the leached mineral. The ENE-WSW Structural trend comprises many granite intrusions crosscut by different hydrothermal injections and consequently several alteration processes. This example between our hands is the more uranium fertile part in El Sela area. Hence, we have carried out mineralogical and chemical studies as well as detailed field geology followed by manual trenching to follow and understand the behavior of the uranium and thorium in the whole rock.

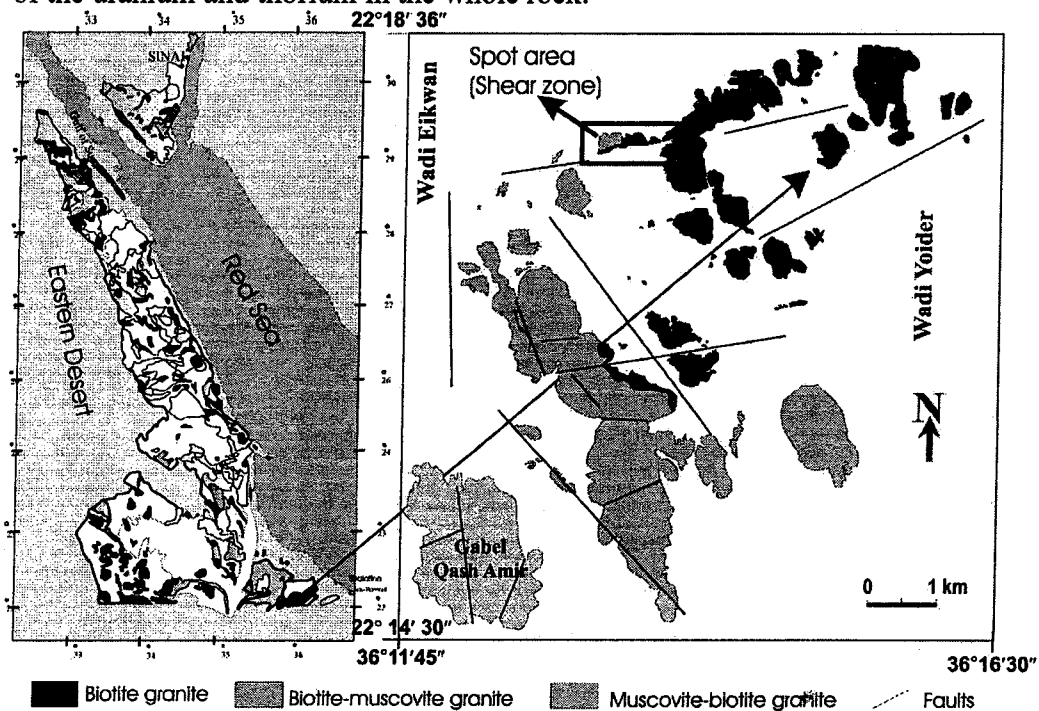


Fig. (1) The shear zone in El Sela granite

## URANIUM POTENTIALITY AND ITS EXTRACTION

### GEOLOGIC AND STRUCTURAL SETTING

Gabal El Sela granites are highly weathered, cavernous and exposed as moderate masses forming an elliptical shaped pluton which is composed of two different granitic magmas. The coarse-grained granite is pink to pinkish gray in color and mainly composed of K-feldspar, quartz, plagioclase, biotite and few muscovite. It rarely contains fine-grained homogeneous enclaves of black color and oval to circular shape. The second type is fine-grained granites are composing of quartz, K-feldspar, plagioclase, biotite and muscovite. It is reddish to pink color and encloses manganese oxide filling joints and fracture as well as disseminating within the rock indicating its highly differentiation nature. Also it is extremely enriched with pyrite and magnetite

The detailed geological studies and field observations exhibit that El Sela area was affected at least by nine successive tectonic events. These events are reflected by high fracture intensity and consequently high weathering and alteration effect.

The ENE-WSW shear zone (fig. 1) dipping  $50^{\circ}$ - $70^{\circ}$  to the south and extending about 9km., with thicknesses varies between 2 to 40m. The ENE-WSW shearing evolved both normal and strike slip movements. Figure (2) represents the detailed map of the western 1400m of this zone. The influence of this trend to the successive tectonic and mineralization events makes its evolutionary history a good example to describe the geologic and tectonic history of El Sela area. The suggested geologic events correlated with the structural evolution and their associated criteria are concluded in chronological sequence as the following:

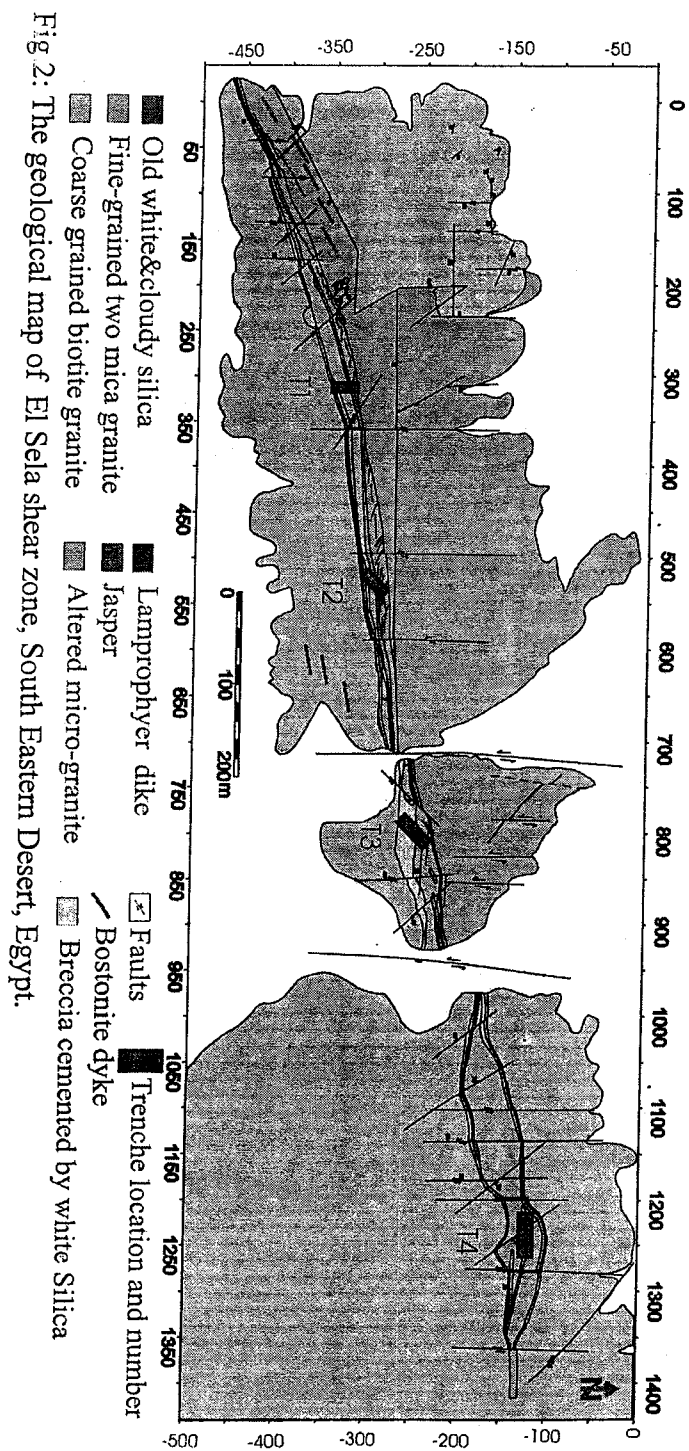


Fig.2: The geological map of El Sela shear zone, South Eastern Desert, Egypt.

## URANIUM POTENTIALITY AND ITS EXTRACTION

During the first two activations, the coarse grained granitic magma was crosscut by the fine-grained two-mica granite. The third reactivation is presented by white massive quartz, it is barren except little amazonite and sulphide crystals only in cloudy patches. During the fourth activation this zone was injected by 1-4m thickness of micro-granite rich in sulphides which dissolved leaving their vugs and completely altered to light green bleached illite. During the fifth reactivation, the shear zone was injected by highly radioactive beige to pink jasper of thickness varying from 20 to 80cm. The sixth and seventh reactivations are contemporaneous with discontinuous exposed basic and lamprophyre dykes of variable thicknesses between 20cm and 3m. The lamprophyre is mainly composed of large alkali feldspar crystals embedded in a fine basic amygdaloidal groundmass rich in calcite. It has higher U-content (40ppm eU) several times greater than that of the ambient granite (Ibrahim et al., 2005). Most alkali feldspar and calcite crystals were disappeared leaving their boxworks forming a possible local trap that is sometimes filled with secondary uranium minerals.

All the previous types of injections were hydraulically altered, brecciated and cemented by the white silica injection which representing the eighth reactivation. Finally, the bostonite dykes crosscut through the ENE-WSW and N-S directions contemporaneous to the ninth reactivation phase. The bostonite was rich with fluids which are indicated by the enclosed alteration halos and acted as heat engine.

Eventually these injections might played an important role as heat, CO<sub>2</sub> and fluids source which may have led to U- mobilization and reconcentration.

As a result of the numerous rejuvenations, many alteration processes are observed throughout the shear zone. Intensive alteration of the micro-grained granite resulted in bleached illite and formation of secondary fluorite and amazonite as well as the complete dissolution of its sulphides leaving their boxworks. Hematitization as red staining, is observed mainly near the bostonite dykes. Episyenitization has been discovered only in the vicinity of the contacts between the two granitic intrusions and is generally superimposed by K-metasomatism associated with traces of violet fluorite.

The highest radioactive anomalies comprising uranophane and anthozonite are incorporated within silicified argillic clayey matrix of the micro-grained granite and the altered lamprophyre dyke of the shear zone. The uranium contents attain values about 3000eUppm with relatively high thorium content, up to 300eThppm which may suggest adding new radioactive elements during the different injections.

Ibrahim, T.M.M. et al.

Lastly, the ENE-WSW shear zone was intersected by the common N-S left-lateral strike slip fault system that resulted by the nearly N-S compression. This trend represents an important tectonic event that controls micro-granite, quartz, lamprophyre and bostonite dykes in the area. all of these dykes are highly radioactive and some of them are associated with uranium mineralization. As a result we can conclude that the complicated geologic and tectonic history of the area represent a promising surface criteria for U-fertility which need to continue an exploration work.

#### TRENCHING AND SAMPLING:

Along the ENE-WSW shear zone some sites were chosen for manual trenching based on a notable radioactivity measurements. The main lithologies in most trenches is variably sized alluvium sediments at the top followed down by chloritized breccia, with clayey matrix very rich with the boxwork vugs of dissolved sulphides.

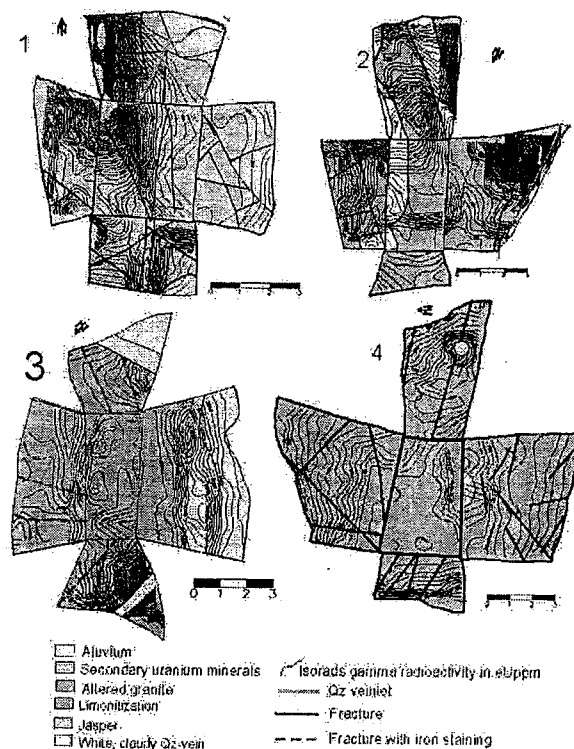


Fig. 3: Geological and radiometric map sketches of excavated trenches on the hot radioactive spots along El Sela mineralized shear zone .

## URANIUM POTENTIALITY AND ITS EXTRACTION

This matrix is cemented by various-colored silica injections. The radioactivity was measured systematically on grid pattern constructed for the trenches using well calibrated and shielded gamma-ray spectrometer (model GS-256). The radioactivity shown, in the isorad sketches (Fig 3-1, 2, 3, 4) is mainly associated with the clay-rich matrix and the beige to pink jasper which is hydraulically brecciated and cemented by white massive silica. Samples are collected from the trenches dump to serve the mineral chemistry and leaching studies

The radioactivity of clay-rich matrix reach up to 2500ppmeU in some spots where anthozonite and secondary U-minerals have been observed with relatively high Th content (200ppm eTh), compared to the background values in enclosing rocks (35 to 40ppmeTh). This indicate that the clay rich matrix may derived from the alteration of a former late magmatic intrusion which was enriched in Th, like to the micro-granite. The locally high radioactivity along the walls of the mineralized clay rich matrix, indicating the percolation of iron-rich oxidizing solutions and this may have been favorable for uranium transportation. The radioactivity of the brecciated jasper ranges between 140 and 1400ppmeU mainly concentrated in the highly rubefacient zones.

### THE MINERAL CHEMISTRY

The microprobe analyses were carried out for some diagnostic radioactive minerals which were identified previously by the scanning electron microscope at CREGU institute, Nancy, France (Fig.4). The analyses show the presence of pitchblende (4, a&b) which has been variably altered producing an hexavalent uranium minerals. Ca-bearing phosphate as autunite (Fig. 4, c&d&e&f&g), Ca-bearing silicate as uranophane as well as a mixture of uranium silicate as coffenite (Fig. 5) are the main hexavalent uranium. Table (1) comprises the microprobe analyses of the identified uranium minerals.

Ibrahim, T.M.M. et al.

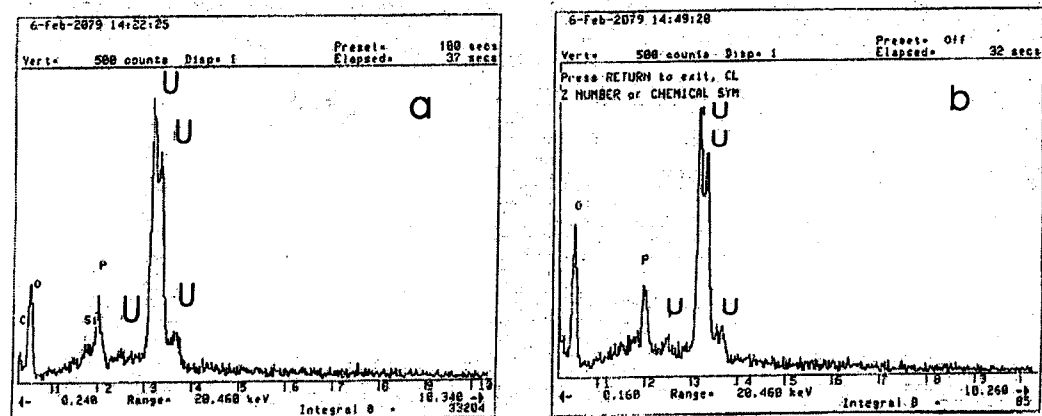
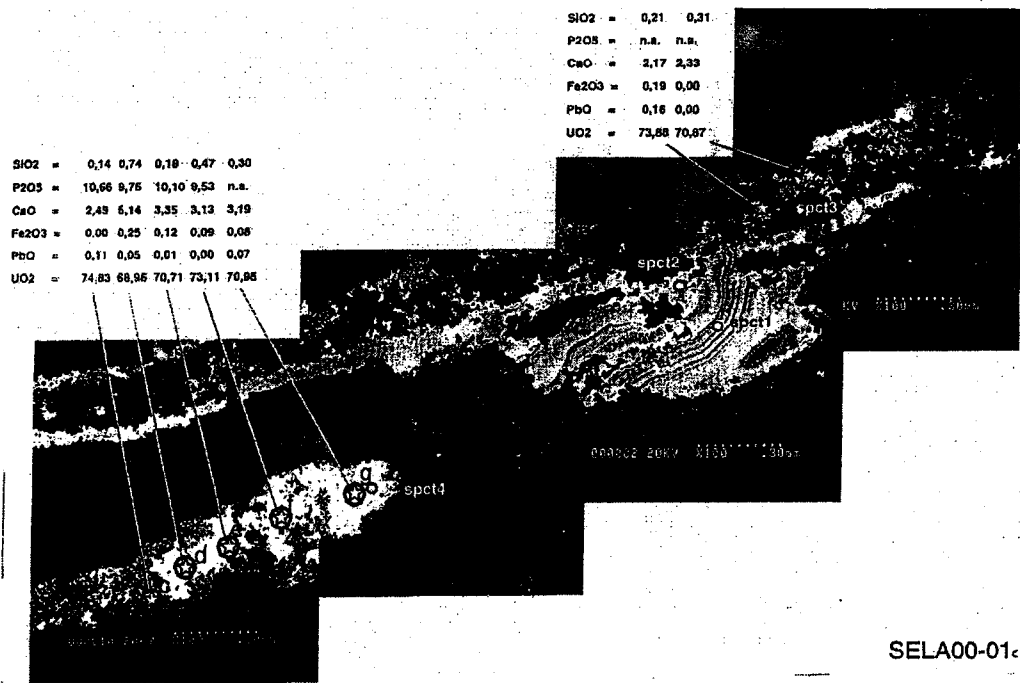


Fig.4: are scanning electron microphotographs, (a,b) are spot analyses of pitchblende with their X-ray emission lines, (c,d,e,f,g) are spot analyses of autonite mineralization from El Sela shear zone.



# URANIUM POTENTIALITY AND ITS EXTRACTION

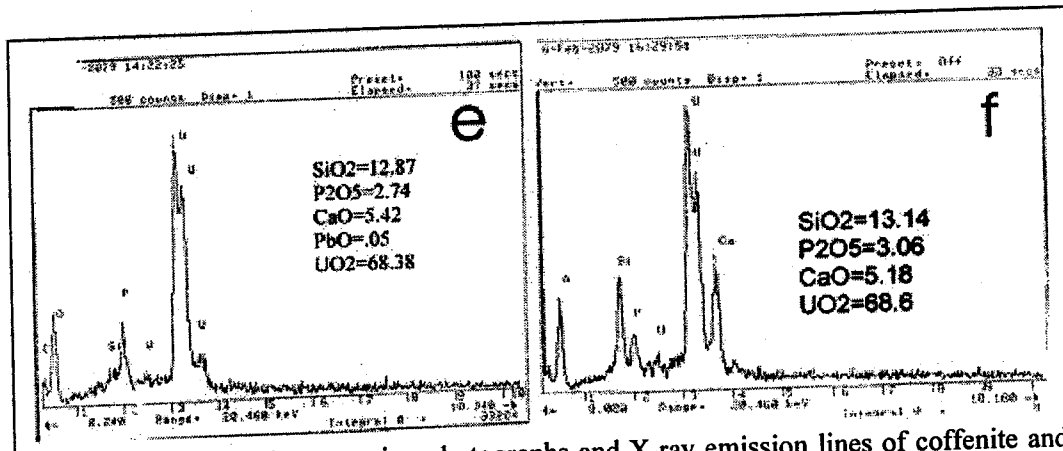
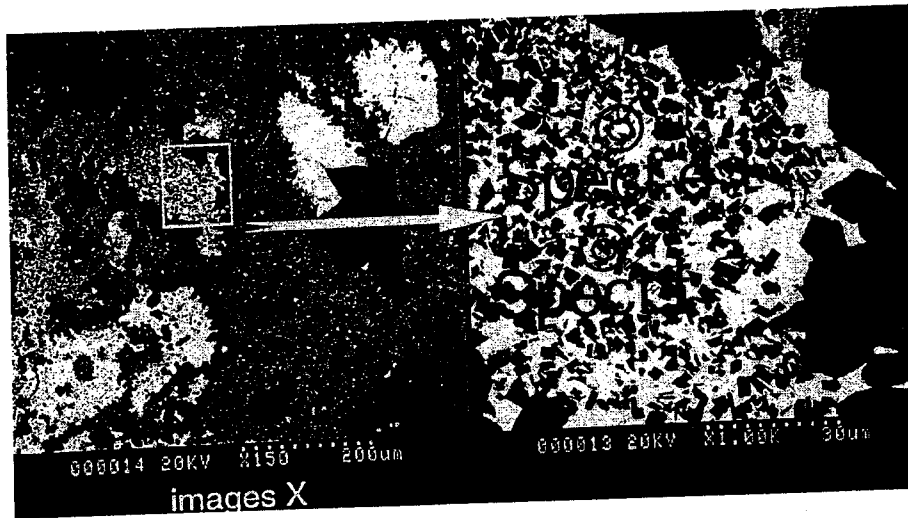


Fig. 5: are scanning electron microphotographs and X-ray emission lines of coffenite and uranophane mixture mineralization from El Sela shear zone.

Table (1): The micro-analyses of the uranium minerals from El Sela shear zone

| Lable   | (Al) | (Si)  | (P)   | (Ca) | (Fe) | (Pb) | (Th) | (U)  | Total | Mineral     | spectrum |
|---------|------|-------|-------|------|------|------|------|------|-------|-------------|----------|
| *S-1-1  | 0.00 | 0.21  | 0.00  | 2.17 | 0.19 | 0.16 | 0.00 | 73.8 | 76.61 | pitchblende | a        |
| *S-1-2  | 0.00 | 0.31  | 0.00  | 2.33 | 0.00 | 0.00 | 0.05 | 70.8 | 73.57 | pitchblende | b        |
| *S-1-4  | 0.00 | 0.30  | 0.00  | 3.19 | 0.08 | 0.07 | 0.00 | 70.9 | 74.59 | pitchblende |          |
| **S-1-5 | 0.00 | 0.47  | 9.53  | 3.13 | 0.09 | 0.00 | 0.04 | 73.1 | 86.38 | Autunite    |          |
| **S-1-6 | 0.02 | 0.18  | 10.10 | 3.35 | 0.12 | 0.01 | 0.00 | 70.7 | 84.49 | Autunite    |          |
| **S-1-7 | 0.00 | 0.74  | 9.76  | 5.14 | 0.25 | 0.05 | 0.01 | 68.9 | 84.92 | Autunite    |          |
| **S-1-8 | 0.00 | 0.14  | 10.66 | 2.49 | 0.00 | 0.11 | 0.00 | 74.8 | 88.24 | Autunite    |          |
| S-2-1   | 0.06 | 12.87 | 2.74  | 5.42 | 0.07 | 0.05 | 0.00 | 68.3 | 89.59 | uranophane  | e, f     |
| S-2-2   | 0.05 | 13.07 | 2.63  | 2.80 | 0.00 | 0.14 | 0.00 | 69.8 | 88.59 | Coffenite   |          |
| S-2-3   | 0.03 | 13.14 | 3.06  | 5.18 | 0.13 | 0.00 | 0.00 | 68.6 | 90.13 | Uranophane  |          |
| S-2-4   | 0.04 | 13.37 | 2.27  | 3.85 | 0.04 | 0.13 | 0.01 | 68.7 | 88.50 | Coffenite   |          |
| S-3-1   | 0.01 | 12.74 | 1.78  | 4.05 | 0.04 | 0.03 | 0.05 | 67.8 | 86.60 | Uranophane  |          |
| S-3-2   | 0.03 | 12.37 | 2.34  | 4.03 | 0.35 | 0.01 | 0.00 | 69.7 | 88.86 | Uranophane  |          |
| S-3-3   | 0.06 | 12.93 | 2.12  | 5.60 | 1.19 | 0.14 | 0.00 | 70.9 | 92.97 | Uranophane  |          |
| S-3-4   | 0.03 | 12.93 | 2.13  | 4.88 | 0.48 | 0.03 | 0.00 | 68.6 | 89.07 | Uranophane  |          |
| S-3-5   | 0.03 | 12.65 | 2.08  | 4.05 | 0.90 | 0.03 | 0.00 | 71.9 | 91.74 | Uranophane  |          |
| S-3-6   | 0.00 | 12.88 | 2.26  | 3.06 | 1.66 | 0.06 | 0.00 | 69.2 | 89.19 | Uranophane  |          |
| S-3-7   | 0.02 | 12.33 | 1.91  | 4.23 | 0.23 | 0.05 | 0.02 | 71.8 | 90.65 | Uranoph     |          |
| S-3-8   | 0.05 | 12.0  | 2.05  | 2.89 | 0.14 | 0.05 | 0.00 | 68.8 | 86.05 | Coffenite   |          |
| S-3-9   | 0.02 | 13.19 | 2.46  | 1.62 | 0.13 | 0.03 | 0.00 | 69.3 | 86.80 | Coffenite   |          |
| S-3-10  | 0.00 | 13.51 | 2.39  | 1.72 | 0.07 | 0.06 | 0.00 | 70.7 | 88.53 | Coffenite   |          |
| S-3-11  | 0.02 | 12.74 | 2.99  | 6.83 | 0.06 | 0.02 | 0.00 | 66.0 | 88.74 | uranopha    |          |
| S-3-12  | 0.04 | 13.42 | 2.45  | 2.08 | 0.03 | 0.11 | 0.04 | 68.7 | 86.90 | Coffenite   |          |

-\*The three first analyses correspond to oxidized pitchblende from which lead has been totally removed by oxidation.

-\*\*The next four analyses correspond to a phase similar to autunite.

-The others are correspond to a phases similar to coffenite and uranophane.

### URANIUM RECOVERY PROCEDURE

A representative technological sample of the uraniferous rock materials was collected for leaching experiments to determine the degree of leachability and subsequent U-recovery from the obtained liquors. Uranium was recovered using anionic exchange resin. The conditions and the efficiency of the leaching and recovery of such ore has been obtained. The resultant product is a bright yellow precipitate (yellow cake) of  $\text{Na}_2\text{U}_2\text{O}_7$  composition. In addition, a tentative flow-sheet was proposed and described.

The study sample was properly prepared for complete chemical analysis to determine its major oxides as well as its uranium contents which assays 950ppmU. Table (2) summarizes the analyses obtained from El Sela technological sample. The high contents of  $\text{Al}_2\text{O}_3$ ,  $\text{Fe}_2\text{O}_3$ ,  $\text{TiO}_2$ , and L.O.I reflect an intensive alteration of the sulphide-rich microgranite into a clayey matrix. Also the low

## URANIUM POTENTIALITY AND ITS EXTRACTION

content of SiO<sub>2</sub> although the presence of numerous silica injections indicates a high potential of dissolution processes affected the shear zone.

Table (2): Chemical composition of El Sela uraniumiferous technological sample.

| Oxides                         | Wt %  |
|--------------------------------|-------|
| SiO <sub>2</sub>               | 70.42 |
| TiO <sub>2</sub>               | 1.26  |
| Al <sub>2</sub> O <sub>3</sub> | 17.15 |
| Fe <sub>2</sub> O <sub>3</sub> | 5.11  |
| MnO                            | 0.75  |
| MgO                            | 1.1   |
| CaO                            | 0.6   |
| Na <sub>2</sub> O              | 0.07  |
| K <sub>2</sub> O               | 1.08  |
| P <sub>2</sub> O <sub>5</sub>  | 0.22  |
| L.O.I                          | 2.24  |
| Total                          | 100%  |

### ACIDIC AGITATION LEACHING:

The conventional acidic agitation leaching technique was carried out on 50g rock sample grinded to a -200 mesh size. The leaching experiments, were performed at different time periods, different temperatures and different solid liquid (S/L) ratios. The obtained slurry was filtered and the left residue was thoroughly washed by a distilled water. The filtrate and washes (leach liquor) were then analyzed for its uranium content. The residue was dried at 110 °C, weighed, ground and analyzed for any possible unleached U.

The mineralogical composition of the study rock material includes mainly uranophane (Table 3), in addition to some other gangue minerals comprises sulphate and iron.

However, acid agitation leaching process depends largely on a number of factors, acid type and concentration, agitation time, leaching temperature, particle size, oxidation state and solid /liquid ratio (S/L). To study the effect of these factors upon the study sample, different series of leaching experiments have been applied.

### EFFECT OF ACID TYPE:

All the mineral acids can dissolve U under certain conditions with different efficiencies. The effect of acid type upon U dissolution efficiency was studied by using 200g/l H<sub>2</sub>SO<sub>4</sub>, HCl and HNO<sub>3</sub> while fixing the other experimental conditions (S/L ratio 1/2, 4hrs, room temp.). U-leaching efficiency was 36.8, 24.3

Ibrahim, T.M.M. et al.

and 29.5 % respectively. The obtained results prove that H<sub>2</sub>SO<sub>4</sub> has achieved the highest U-leaching efficiency (36.8 %).

Table (3): X-Ray diffraction pattern for uranophane

| Sample |      | Uranophane ASTM# (8-442) |      |
|--------|------|--------------------------|------|
| dA°    | I/I° | dA°                      | I/I° |
| 7.83   | 100  | 7.88                     | 100  |
| 5.37   | 20   | 5.42                     | 40   |
| 4.75   | 22   | 4.76                     | 50   |
| 3.92   | 61   | 3.94                     | 90   |
| 3.58   | 28   | 3.6                      | 40   |
| 3.47   | 24   | 3.41                     | 10   |
| 3.19   | 25   | 3.2                      | 50   |
| 2.97   | 18   | 2.99                     | 80   |
| 2.88   | 26   | 2.91                     | 80   |
| 2.67   | 23   | 2.69                     | 40   |
| 2.62   | 21   | 2.63                     | 50   |
| 2.19   | 13   | 2.2                      | 40   |
| 2.09   | 15   | 2.1                      | 50   |
| 1.97   | 15   | 1.97                     | 70   |
| 1.9    | 12   | 1.91                     | 20   |
| 1.76   | 11   | 1.77                     | 30   |
| 1.74   | 13   | 1.75                     | 30   |
| 1.71   | 12   | 1.71                     | 10   |
| 1.58   | 10   | 1.58                     | 20   |

#### **EFFECT OF H<sub>2</sub>SO<sub>4</sub> CONCENTRATION:**

The effect of H<sub>2</sub>SO<sub>4</sub> concentration upon the dissolution efficiency of U for the studied sample was tested using different acid concentrations ranging between 100 and 300 g/l while other variables were kept constant (S/L ratio ½, 4hrs, room temp.). The leaching efficiencies of uranium versus acid concentrations are plotted in (Fig.6a). The obtained results clarifies the increasing of dissolution U-efficiency of with increasing H<sub>2</sub>SO<sub>4</sub> concentration, from 22.4 % at 100 g/l H<sub>2</sub>SO<sub>4</sub> up to 71.4 % at 300 g/l H<sub>2</sub>SO<sub>4</sub>.

#### **EFFECT OF AGITATION TIME:**

The effect of agitation time against the efficiency of U-dissolution was measured at different time periods ranges between 2 and 10 hours (hrs) using 300 g/L H<sub>2</sub>SO<sub>4</sub> while the other factors were kept constant (S/L ratio ½, room temp.). The obtained results ( Fig.6b) shows that U dissolution efficiency increased with increasing the agitation time till 8 hrs and then no improvement.

#### **EFFECT OF LEACHING TEMPERATURE:**

The effect of different leaching temperature upon the efficiency of U-dissolution for the studied sample has been calculated using 300 g/l H<sub>2</sub>SO<sub>4</sub> for 4 hrs agitation times at S/L ratio of 1/2. The obtained results in (Fig.6c) reflect a positive correlation where the U dissolution efficiency increased from 71.4 to 95.8

## URANIUM POTENTIALITY AND ITS EXTRACTION

% with increasing leaching temperature from room temperature (about 35 °C) to 100 °C. So, it can be concluded that the refractory minerals (e.g monazite and zircon) were dissolved beside the secondary ones at elevated temperatures. This means that about 24.4% of the U-contents in the studied sample were hosted in refractory minerals.

### EFFECT OF SOLID / LIQUID RATIO:

The effect of S/L ratio upon the U-dissolution efficiency was studied in the range of 1/1 to 1/4 using 300g/l H<sub>2</sub>SO<sub>4</sub>, 4hrs as leaching time and 100 °C as leaching temperature. The obtained results as shown in (Fig.6d) proved the inverse relation between them where at S/L ratio of 1/1 the U leaching efficiency was 60.6%, by decreasing the S/L ratio to 1/4, U leaching efficiency increases to 74.4%. On the other hand it is noticed that decreasing the S/L ratio beyond 1/2 resulting a slight increase in U dissolution efficiency. So, it can be stated that the S/L ratio of 1/2 is the optimum one.

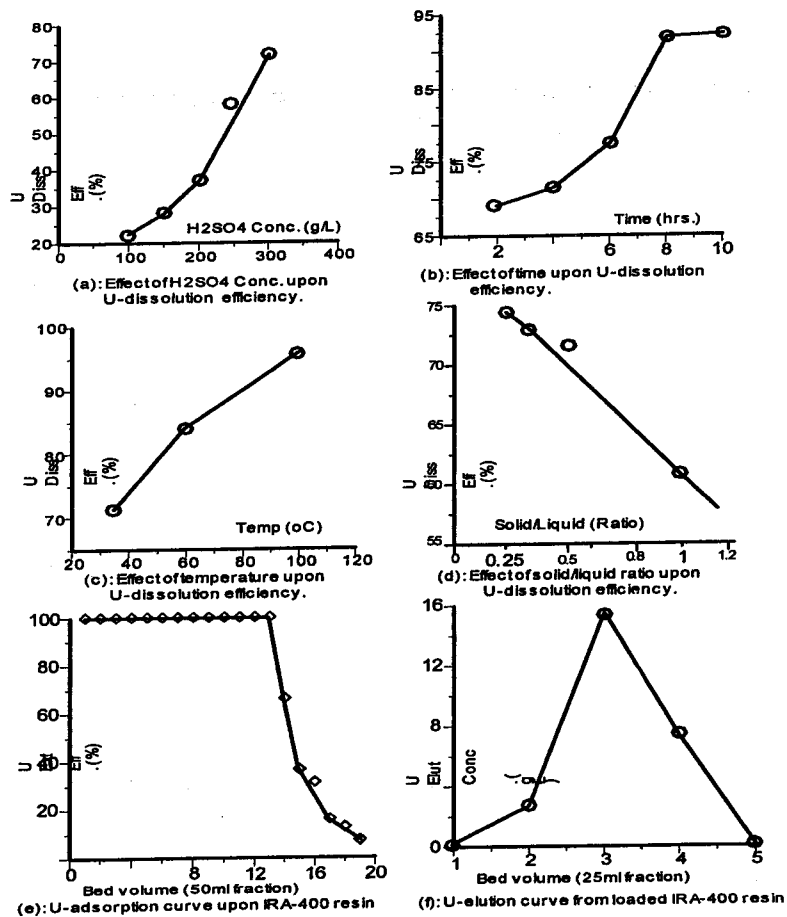


Fig.6: Uranium dissolution efficiency against the different factors.

**Ibrahim, T.M.M. et al.**

#### **EFFECT OF GRAIN SIZE AND OXIDATION CONDITIONS:**

Since the U content of the studied sample has been completely leached (95.8%) without minimizing the grain size to more than -60 mesh and without adding any oxidizing agent, it seems unnecessary to study these two factors. The authors believe that the presence of most of uranium content in the form of secondary uranium minerals and/or the presence of sufficient manganese and iron oxides could act as natural powerful oxidizing agents.

From the foregoing acidic agitation leaching results of the study ore material, it can be concluded that the optimum leaching conditions are:

- H<sub>2</sub> SO<sub>4</sub> Conc.: 300 g/l
- Agitation time: 8 hrs
- Leaching temperature: room temp.
- Solid/liquid ratio: 1/2

#### **U-EXTRACTION EXPERIMENTS:**

In general, uranium recovery from its pregnant leach liquors is commonly performed by one or more of the three known techniques namely; ion-exchange resins, solvent extraction and direct precipitation. Choice of the suitable method for the recovery of U depends primarily upon its concentration in the leach liquor, the amount and concentration of the co-dissolved impurities as well as upon the desired final product purity.

#### **U-ADSORPTION:**

In this work, after conducting the solubilization of U from the study rock material by acidic agitation leaching method using H<sub>2</sub>SO<sub>4</sub>. The uranium extraction from such sulphate leach liquor was achieved by the most commonly used technique namely anion-exchange resin via a column (100ml height & 1cm diameter) backed with 9.7ml wet settled resin (wsr) Amberlite IRA – 400.

The leach liquor of the composition given in table (4) was firstly adjusted to pH 1.7 using 10% NaOH and passed downwards the resin at fixed flow rate of 0.2 ml/min which corresponds to a retention time of 19.4 minute. Fig. (5e) show the U adsorption results which indicate that the U adsorption efficiency attained 72.8% and the loaded U content upon the used column attains 0.66g. This corresponds to a capacity of about 68 gU/l WSR. Referring to the resin theoretical capacity determined by (El-Hazek, 1965) of 1.56 meq/ml WSR while gives for the U tetravalent tri-sulphate complex a capacity of about 92.8 gU/l WSR. The attained capacity in this work represent about 73.3% of the theoretical capacity. The relatively low capacity in spite of the high contact time used ( 19.4 minutes ) could be interpreted as due to the relatively low U content relative to sulphate and

## URANIUM POTENTIALITY AND ITS EXTRACTION

iron concentrations (Table 4) and hence, the Fe and some other elemental species will be co-adsorbed with U.

Table (4): Chemical composition of the prepared pregnant solution from El Sela uraniferous ore material.

| Component                      | Concentration (g/l) |
|--------------------------------|---------------------|
| U                              | 0.91                |
| Fe <sub>2</sub> O <sub>3</sub> | 2.73                |
| SO <sub>4</sub> --             | 33.8                |
| pH                             | 0.8                 |

### U-ELUTION:

On the other hand with respect to the elution of U from the loaded resin, chloride system eluant (1M NaCl acidified with 0.15 N H<sub>2</sub>SO<sub>4</sub>) was used. The eluant passed downwards the loaded resin with a flow rate of 0.2 ml/min and a retention time of 19.4 minutes. The elution results as shown in (Fig. 5f) indicate that the elution efficiency was 97.2%. The latter has been achieved after passing about 5 bed volumes while the effluent solution attained as low as 55ppmU. The fractions of high U content will be directed to the precipitation circuit.

### SODIC DECOMPOSITION:

In order to prepare a U sample product from the study rock material, the eluted uranium fractions were collected and then precipitated by sodic decomposition. The collected uranium eluate solution was heated at 70 °C and then 10% NaOH was added till pH 5-6.5. A bright yellow precipitate (yellow cake) of sodium di-uranate (Na<sub>2</sub>U<sub>2</sub>O<sub>7</sub>) was obtained. After drying, analysis of a sample product resulted in 60% U equal to ~70.74% U<sub>3</sub>O<sub>8</sub> and 5% water of crystallization (the minimum considered U<sub>3</sub>O<sub>8</sub>= 65 w %, Ritcey, 1993). Based on the chemical formula of sodium di-uranate, the precipitation efficiency amounted to about 80%.

Finally a tentative flow sheet is proposed for the treatment of the worked uraniferous rock material (Fig.7) starting with acidic agitation leaching using H<sub>2</sub>SO<sub>4</sub> and ended with uranium precipitation as Na<sub>2</sub>U<sub>2</sub>O<sub>7</sub> which was identified by Scanning Electron Microscope(Fig.8) .

Ibrahim, T.M.M. et al.

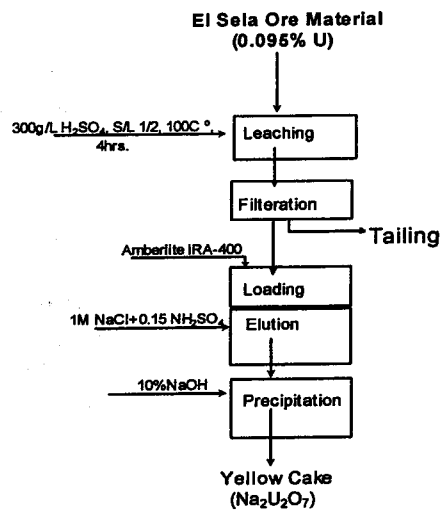


FIG.7: Proposed flow sheet for U-recovery from El Sela uraniferous technological sample.(heating to 100° c is excluded when the agitation time exceeds to 8hrs)

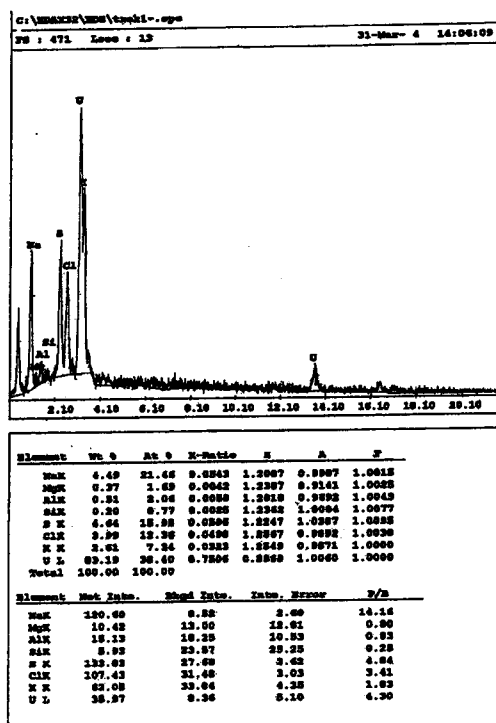


Fig.8: Scanning Electron Microscope EDX spectrum for the yellow cake end product.



## URANIUM POTENTIALITY AND ITS EXTRACTION

It is worthy to mention herein that, uranium in the studied sample or in the different working streams or else the final product was spectrophotometrically analyzed using Arsenezo III method (Marczenko, 1986).

### DISCUSSION AND CONCLUSIONS

The present study on El Sela shear zone reached to some important indications. Primarily, El Sela granite comprise different granitic magmas. It have an extensive late magmatic injections contemporaneous with repeated tectonic activities along the ENE-WSW and N-S trends. These injections were associated with high fluid phases as indicated by successive alteration processes and consequently U-redistribution.

The microprobe analyses proved the presence of easily leachable (low thorium) primary uranium mineral represented by pitchblende as well as autonite, coffenite and uranophane as secondary uranium minerals.

Some features indicate that the late hydrothermal activities in the mineralized shear zone (ENE-WSW) played an important role in exceeding the U-potentiality. These features are summarized as follow:

- 1- The abundance of lead, indicating an old mineralization, but has been leached from the primary uranium minerals due to the surface oxidation.
- 2- The occurrence of strongly altered microgranite within the shear zone.
- 3- The simultaneous increase of thorium with uranium determined by ground spectrometric measurements which showing as much as 250hppmeTh correspond to 3000ppmeU. Such features clearly indicate the percolation of late high potential fluid phases in the shear zone. These fluids leading to the simultaneous enrichment of uranium, thorium and may other minerals (Cuney, 2001). Such an enrichment has been also observed from the geochemical analyses of El Missikat silica vein and the illite zone (Ibrahim, 2002).
- 4- The disequilibrium between the equivalent ( $>2500\text{ppmeU}$ ) and the elemental uranium (950ppm) assures that the majority of the U may concentrated at depth in the ENE-WSW shear zone which acts as good channel and trap.

With respect to U recovery, it can be concluded that the optimum U dissolution efficiency has been achieved after conducting 300g/l  $\text{H}_2\text{SO}_4$  upon the study rock material in a manner to have a S/L ratio of 1/2, 4hrs as leaching time and 100 °C as pulp temperature or 8hrs leaching time at room temperature.

U extraction from the prepared sulphate leach liquor was investigated via a column backed with Amberlite IRA-400 anion-exchange resin. The obtained relatively low working capacity of the study resin (68gU/l WSR) in spite of the

Ibrahim, T.M.M. et al.

high contact time (19.4 minutes) may be due to the relatively low U content relative to sulphate and iron concentrations in the prepared sulphate leach liquor. On the other hand, the U elution efficiency in this work attained 97.2% while the fractions of high U content were subjected to sodic decomposition to precipitate uranium using 10%NaOH solution at pH 5-6.5. The produced yellow cake was in the form of  $\text{Na}_2\text{U}_2\text{O}_7$ . Chemically, it is considered as a marketable product where its U content assays 60% and 5% water of crystallization.

Thus, the surface studies on the ENE-WSW shear zone yield a favorable environment to form uranium deposit and the area still needs more subsurface investigation through exploratory drill holes to complete the exploration programme.

## REFERENCES

- Abdel Meguid A. A.; Ammar, S. E; Ibrahim, T. M. M.; Ali Kh. G.; Shahin, H. A.; Omer S. A; Gaafar I. M. E.; Masoud S. M.; Khamis, A. A.; Haridy, M. H.; Kamel, A. I.; Mostafa, B. M.; Abo Donia A.; Abdel Gawad, A. E.; Aly E. M. (2003): Uranium Potential of Eastern Desert Granites, Egypt. NMA report for Model project EGY/03/014 sponsored by IAEA 270P
- Cuney M., 2001: Uranium resource development in the Eastern Desert of Egypt, Metallogenic studies of the granite. IAEA-TCR 00456 Report, Department of technical co-operation.
- Cuney M., Friedrich M., Blumenfeld P., Bourguignon A., Boiron M. C., Vigneresse J. L. and Poty B., (1990): Metallogenesis in the French part of the Variscan orogen. Part 1: U preconcentrations in pre-Variscan and Variscan formation-a comparison with Sn, W and Au. *Tectonophysics*, 177: 39-57.
- El Hazek, N. M. T. (1965): Studies on the leachability and uranium concentration of El-Atshan and comparable ores in relation to mineralogical composition, M. Sc. Thesis, Ein Shams Univ., Egypt.
- Ibrahim T.M., 2002: Geologic and Radiometric Studies of the Basement-Sedimentary Contact in the Area West Gabal El Missikat, Eastern Desert, Egypt., Ph. D. Thesis, Fac. Of Scie., Mansoura University, 214p.
- Ibrahim, T. M. M.; Cuney, M.; Ali, K. G.; Abdel Meguid, A. A; Gaffar, I, M.; Shahin H.; Omar, S. A., Masoud, S. M.; Haridy, H. M.M., 2005: The U-fertility Criteria Applied to El Sela Granite, South Eastern Desert, Egypt. International Symp. Uranium Production and Raw Materials for the Nuclear Fuel Cycle, IAEA, Vienna, Austria, 20-24 June 2005, pp. 100-103.
- Marczenko, Z. (1986): Separation and spectrophotometric determination of elements, Ellis Horwood Limited Publishers. Chicester, John Wiley and Sons, New York.
- Ritcey, G.M.(1993): Uranium extraction technology, Tec. Rep. Ser. No. 339, IAEA, Vienna.